

# Attractions in Sterically Stabilized Silica Dispersions

## II. Experiments on Phase Separation Induced by Temperature Variation

J. W. JANSEN, C. G. DE KRUIF, AND A. VRIJ

*Van't Hoff Laboratory for Physical and Colloid Chemistry, University of Utrecht, Padualaan 8, 3584 CH Utrecht, The Netherlands*

Received September 2, 1985; accepted January 28, 1986

On lowering the temperature initially homogeneous dispersions (in a variety of solvents) of silica coated with octadecyl chains show a separation into two phases of different concentration. The temperature of first instability is not strongly correlated with the solubility parameter of the solvent. Phase diagrams have been constructed for two dispersions in toluene and one in benzene. It is found that phase separation temperatures decrease with decreasing particle size. The concentration of the phases show a dependence on overall concentration. For the dilute phase this is in qualitative agreement with theoretical calculations for polydisperse systems. © 1986 Academic Press, Inc.

### 1. INTRODUCTION

In our laboratory we studied model colloidal particle systems in which the particle interaction can be described as a so-called hard sphere interaction (1, 2). These colloidal systems contain silica particles coated with octadecyl chains and are dispersed in cyclohexane or chloroform. An extension of this work is to search for particles that have other types of interactions, e.g., an attraction part in the interaction potential. Since we know that the silica particles cannot be dispersed in all solvents, we expected that in certain solvents silica would be only partially soluble and this proved to be the case. The solvent quality can be varied easily by changing temperature or pressure. The same holds for polymer solutions.

The interaction forces between polymer coated particles depend on the quality of the solvent with regard to the stabilizing chains (3–5) and on the London–Van der Waals forces between the particle cores. In the case of our silica particles these dispersion forces are weak (6). The quality of the solvent with regard to the chains can be termed bad, fair,

or good. The interactions in good solvents are repulsive, because the chain segments prefer contacts with solvent molecules to contacts with chain elements of other particles (this is called steric stabilization). In bad solvents the situation is reversed and the interaction between the chains is therefore attractive. For intermediate solvents the stability is a very delicate matter, because the interaction (free) energy must be compared with the thermal energy ( $kT$ ). With polymer coated particles, there are numerous contacts between the chains and therefore slight differences in the chemical nature of the solvent and chain may lead to large differences in stability. The chemical nature of a solvent depends on temperature and pressure, so variation in these can cause a change in stability. The interaction between two polymer layers is correlated with the solubility of free polymer, which can be described by means of solubility parameters and theta temperature.

As mentioned above, the silica dispersions we use contain spherical particles with a very dense layer of short, aliphatic chains attached terminally to the silica core. Although these chains are much shorter than a polymer chain

we expect the same mechanism of interaction. In a good solvent (e.g., cyclohexane), where the chains are solvated with solvent molecules, a slight interpenetration of two stabilizing layers leads to a strong repulsion, which is modeled as a hard sphere interaction. The repulsion is very strong because the chains are short, uniform in length, and cover the surface densely. The number of contacts is much smaller than with polymer stabilized systems since the chains are much shorter and because our particles are rather small. Because of the relatively low number of contacts the interaction between two particles as a function of solvent quality does not change as much as with polymer coated particles. We think therefore that our silica system is a very suitable one for investigating the effects of attractions in colloidal dispersions, since the interaction potential can be varied from a hard sphere repulsive to an attractive one in a relatively large temperature range.

In our systems the attraction is found to increase with decreasing temperature. If the temperature is lowered too much the attraction will be so strong that the particles will tend to stick together permanently. This process is often called flocculation and will not lead to an equilibrium state. With large, polymer coated particles this already begins just below the temperature of first separation, so with such systems only the flocculation temperature can be measured. With our systems there is a large temperature region where equilibrium can be attained. We have therefore measured the composition of the coexisting phases as a function of temperature. A preliminary result was published elsewhere (7). Recently Edwards *et al.* (8) have measured phase separation of silica particles like ours in *n*-alkanes. They found both upper and lower flocculation temperatures. The upper flocculation was attributed to the London–Van der Waals attractions between the particles, as the density of the intervening liquid decreases. We will compare their results with ours.

First the stability of our silica particles in a number of solvents was investigated. Then the

phase separation in benzene and toluene was studied in greater detail.

## 2. PREPARATION AND CHARACTERIZATION OF THE PARTICLE SYSTEMS

We used three samples of silica particles with different radii. The particles were synthesized by a method described by Van Helden *et al.* (9). The synthesis starts with the hydrolysis of tetraethylsiloxane (Fluka) in ethanol and thereafter condensation to amorphous silica occurs in the presence of ammonia and water. The resulting charge stabilized particles are spherical and monodisperse in size. Next a layer of aliphatic chains is grafted onto the surface by esterification with octadecyl alcohol. The excess octadecyl alcohol is removed by vacuum distillation and repeated (ultra) centrifugation in cyclohexane. The resulting product is dispersed in cyclohexane; it can however be dried to a white powder and easily redispersed in other solvents, which shows the intrinsic stability of the system.

Particles were characterized by the following techniques: transmission electron microscopy (TEM), elemental analysis (C, H, and Si), static light scattering, photon correlation spectroscopy (PCS), and ultra centrifugation. In addition the density and the refractive index of the particles were measured. For details of these techniques we refer to (9). Concentration series were made by drying the silica (80°C over a nitrogen stream) and redispersing a known weight in cyclohexane. The characterization results thus obtained are summarized in Table I.

The interactions between the silica particles in cyclohexane are found to be of the hard sphere type (1, 2), i.e., a strong repulsion at particle contact. The interaction potential in other solvents is discussed in (6).

## 3. EXPERIMENTS ON PHASE SEPARATION

### 3.1. *The Quality of Several Solvents with Regard to Coated Silica Particles*

First we studied the dispersability of silica particles (SJ9) in a great variety of solvents.

TABLE I

Particle Characterization by Means of Elemental Analysis, Transmission Electron Microscopy (TEM), Photon Correlation Spectroscopy (PCS), Sedimentation Velocity, Density, and Refractive Index Measurements

Technique	Quantity measured	Code		
		SE2	SJ9	SJ4
Elemental analysis	% w/w Organic layer	10.4	11.7	13.7
TEM	Radius (nm)	37.2	30.9	18.4
	Rel. SD	0.13	0.13	0.18
PCS	Radius (nm)	48	38	26
PCS and sedimentation	$M$ ( $10^8 \text{ g} \cdot \text{mole}^{-1}$ )	3.1	1.7	0.6
	Density ( $\text{g} \cdot \text{cm}^{-3}$ )	1.82	1.75	1.72
	Refractive index ( $\lambda_0 = 546 \text{ nm}$ )	1.440	1.43	1.428

We made dispersions with a concentration of  $0.1 \text{ g} \cdot \text{cm}^{-3}$  by dissolving  $0.5 \text{ g}$  silica in  $5 \text{ cm}^3$  solvent. When necessary the sample was warmed to disperse the silica. For each solvent we recorded the temperature below which the dispersion became unstable. This was done by inspecting the dispersion visually for inhomogeneities. By turning the cuvettes upside down we could observe the flowing or gelling properties of the dispersion. The results are listed in Table II. For the smaller particles (SJ4) the transition temperature in benzene turns out to be  $18^\circ\text{C}$  and in toluene about  $-5^\circ\text{C}$ . Suitable solvents are toluene (for SE2 and SJ9) and benzene (for SJ4), since the transition temperature in these solvents is not too far below room temperature and therefore easily accessible experimentally.

### 3.2. Cloud-Point Temperatures

We measured the temperature at which a dispersion of given concentration starts to separate on cooling. Because at this temperature a very small amount of another (finely divided) phase appears, the turbidity increases sharply and the temperature is therefore called a cloud-point temperature (CPT). We measured the CPT for the system (SJ9) in toluene in the concentration range  $0.01$  to  $0.2 \text{ g} \cdot \text{cm}^{-3}$ . The turbidity (at  $\lambda_0 = 700 \text{ nm}$ ; measured with a Shimadzu spectrophotometer in  $1\text{-cm}$  cu-

vettes) is recorded on cooling the dispersions at a rate of  $1^\circ\text{C}$  per hour. Typical examples are shown in Fig. 1. The point where turbidity sharply increases is taken as the cloud-point temperature. In most cases the change is more gradual. The cloud points are then found from the intersection of the extrapolated curves from the high temperature part (where there is little attraction) and from the low temperature part, which shows a strong increase (because of phase separation). These extrapolations are shown in Fig. 1. In Fig. 2 the experimentally determined cloud-point temperatures are plotted as a function of concentration.

### 3.3. Phase Separation as a Function of Temperature and Concentration

Dispersions of the particles were made by weighing an amount of dried silica in cylindrical cuvettes. A weighed quantity of solvent (toluene for SE2 and SJ9, benzene for SJ4) was added and the weight-concentration of the dispersion was calculated from the densities of solvent and silica. The cuvettes were closed with a screw-cap with a Teflon-coated liner. The inner diameter of the cuvettes was measured in advance.

To obtain a phase diagram (i.e., a representation of the composition of the phases as a function of temperature) one has to measure

TABLE II  
 Dispersability of Coated Silica (SJ9) ( $c \approx 0.1 \text{ g} \cdot \text{cm}^{-3}$ ) in Various Solvents  
 in Relation to the Refractive Index and Solubility Parameter

Solvent	Instability temperature ( $^{\circ}\text{C}$ )	Appearance when unstable	Refractive index ( $\lambda_0 = 580$ )	Solubility parameter ( $\text{cal} \cdot \text{cm}^{-3}$ ) <sup>1/2</sup>
2-Methylbutane	4	<i>a</i>	1.354	6.63 (10)
<i>n</i> -Hexane	4	<i>b</i>	1.375	7.24 (10)
<i>n</i> -Octane	4	<i>a</i>	1.397	7.55 (10)
<i>n</i> -Decane	8	<i>a</i>	1.410	7.72 (10)
<i>n</i> -Dodecane	18	<i>a</i>	1.422	7.83 (10)
<i>n</i> -Tetradecane	23	<i>a,c</i>	1.429	7.9 (11)
<i>n</i> -Hexadecane	29	<i>a,c</i>	1.435	7.93 (10)
Isooctane	8	<i>a</i>	1.392	—
Heptamethylnonane	4	<i>a,c</i>	1.43	—
Cyclohexane	5	<i>c,d</i>	1.43	8.18 (10)
Cyclooctane	4	<i>a,d</i>	1.459	—
<i>trans</i> -Decalin	4	<i>a</i>	1.470	8.8 (11)
Benzene	39	<i>b</i>	1.501	9.15 (10)
Toluene	9	<i>b</i>	1.496	8.91 (10)
<i>p</i> -Xylene	2	<i>a,d</i>	1.496	8.8 (11) <sup>g</sup>
Ethylbenzene	8	<i>a</i>	1.496	8.7 (11)
Diethyl ether	4	<i>b</i>	1.353	7.74 (10)
Octadecyl alcohol	—	<i>e</i>	—	—
Decyl alcohol	—	<i>f</i>	1.437	—
Tetrahydrofuran	-9	<i>a</i>	1.405	9.32 (10)
1,4-Dioxane	—	<i>e</i>	1.422	9.73 (10)
Dichloromethane	48	<i>b</i>	1.424	9.07 (10)
Chloroform	-4	<i>a,c</i>	1.446	9.24 (10)
Carbon tetrachloride	-9	<i>a</i>	1.460	8.58 (10)
Pyridine	36	<i>b</i>	1.510	10.58 (10)
Carbon disulfide	46	<i>b</i>	1.632	10.0 (11)
Octamethylcyclsiloxane	—	<i>e</i>	1.44	—

<sup>a</sup> Shows a liquid filling gel; sample does not flow.

<sup>b</sup> Gives a clear separation into two phases.

<sup>c</sup> Shows hardly any turbidity ( $\Delta n \approx 0$ ).

<sup>d</sup> Solvent freezes.

<sup>e</sup> Does not dissolve at all; solvent remains clear.

<sup>f</sup> Dissolves partly at 100 $^{\circ}\text{C}$ ; solvent becomes turbid.

<sup>g</sup> Value of *o*-xylene.

the concentrations of particles in both phases (dilute and concentrated) after equilibrium at low temperatures has been reached. The simplest and most obvious way to measure a concentration is to take a known volume of the dispersion (e.g., with a pipet), dry it, and weigh the silica left. Unfortunately this method is rather sample (and time) consuming, since large volumes have to be taken in order to obtain accurate results. If small volumes are

used there is always a risk that a small amount of the other phase will be drawn into the pipet, leading to an incorrect concentration. Furthermore, if a concentration gradient is present it is almost impossible to determine the equilibrium concentrations near the interface. Such a gradient may arise when gravitation forces also play a role in the separation, as is observed in critical phenomena in gases. Of course sedimentation of the particles also re-

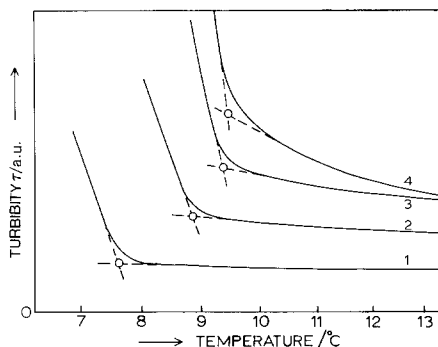


FIG. 1. Estimate of the cloud-point temperature of particles (SJ9) in toluene. The turbidity of samples with concentrations 0.018 (1), 0.039 (2), 0.065 (3), and 0.157 (4)  $\text{g} \cdot \text{cm}^{-3}$  at decreasing temperatures is plotted. The extrapolation to find the CPT (O) is shown.

sults in a gradient. Fortunately we had no problems of this kind, probably because our particles were small.

Because of the above-mentioned problems we have decided to determine the concentration by means of turbidity. The actual measurement of the turbidity must not be done near the phase separation temperature, because then the turbidity is strongly dependent on the temperature (see Fig. 1) and often too high to measure. One therefore chooses a temperature at which the turbidity does not depend strongly on temperature. Apparently this is the case at temperatures 10–20°C above the phase separation temperature.

Because we want to know the concentration at low temperatures (when separated) we must make certain that the phases do not mix on warming toward the temperature at which the turbidity is measured. By warming slowly, convection and thus mixing is avoided. Furthermore convection will be slight because of the difference in the density of the two phases.

In preliminary experiments the samples were simply placed in a water bath which had already been cooled to the desired temperature. Under these conditions the separation into two phases is not very reproducible (e.g., the height of the concentrated phase varies). We also found that cooling the water bath with the samples in it resulted in a smaller volume

of the concentrated phase. This suggests that the phase separation depends on the cooling rate. Measurements of the turbidity of the dilute phase show that its concentration increases with decreasing cooling rate. At rates lower than 1°C per hour no further increase is found. The experiments were therefore done by cooling the samples at a rate of 1°C per hour from room temperature to the temperature at which separation was studied.

In the dilute (upper) phase some silica adheres to the wall of the cuvettes. This silica probably “belongs” to the concentrated phase. On warming to room temperature (where turbidity is measured) this silica “melts” and becomes unstuck. Because of the difference in the density of the concentrated and the dilute phase this silica settles and coalesces with the concentrated phase. However some of this silica may dissolve in the dilute phase, which therefore becomes too concentrated. In order to circumvent this problem, we warmed the samples and cooled them a second time without mixing the contents of the cuvette. The concentration of the dilute phase did not change within experimental error after the second cooling cycle, so the amount of concentrated phase dissolved will be negligible. The concentrated phase however did decrease in volume during the second cooling cycle and its concentration increased. Cooling the cuvettes for a third time did not alter the volume and thus the concentration any further.

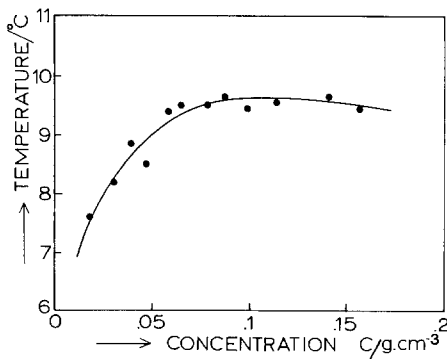


FIG. 2. Cloud-point temperatures against concentration. The drawn curve is to guide the eye.

### 3.4. The Appearance of the Phase Separated Samples

At low temperatures both the dilute and the concentrated phase are milky white. On warming to room temperature the phases become increasingly transparent, although the concentrated phase remains cloudy. The interface between the phases is difficult to observe and locate precisely (because of the high turbidity) at the phase separation temperature, but in some samples it looks rather sharp. On tilting the cuvette the concentrated phase hardly flows due to its own weight. At room temperature (with no attractions) this phase flows easily and the interface is clearly visible. If the separated samples are left at room temperature for about a day the interface becomes less sharp, because the particles diffuse. During the separation experiments the concentration near the meniscus becomes lower as a result of sedimentation ( $\pm 1$  mm per day for SE2 and less for the other particles), but this is only a minor effect and is therefore neglected.

### 3.5. Turbidity Measurements for Concentration Determination

By measuring the turbidity of the samples of known concentrations we obtained calibration curves at 25°C (Fig. 3). The transmission was measured in a setup where a collimated laser beam (He-Ne;  $\lambda_0 = 632$  nm) passed

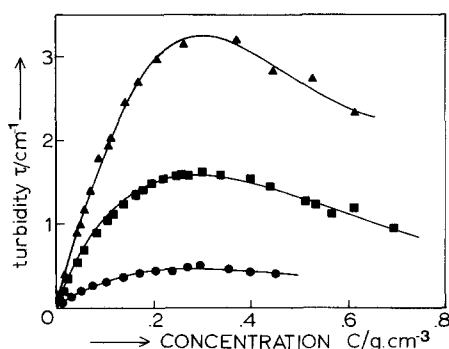


FIG. 3. Calibration curves of SE2 and SJ9 in toluene and SJ4 in benzene at 25°C. The turbidity is plotted against the concentration.

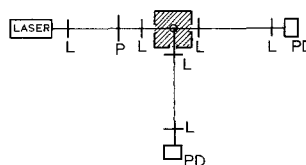


FIG. 4. Setup for measuring turbidity and light scattering at an angle of 90°. The light source is a He-Ne laser; a pinhole (P) and two lenses (L) provide a narrow beam. The cuvette holder is filled with toluene to prevent unwanted reflections. The lenses (L) are placed so that the light is focused into the detectors (PD).

through the cuvette and the transmitted intensity was measured with a photo-diode (Fig. 4). In this setup the light scattered at an angle of 90° can be measured as well. The position of the cuvette can be varied vertically, so the concentration can be measured as a function of height and a concentration gradient (if present) can be measured.

It is clear that near the maximum of these curves and at higher concentrations it is not possible to obtain an accurate measure for the concentration. The concentration of the concentrated phase ( $c''$ ) will always lie in this region of the calibration curve and cannot be determined from turbidity. To obtain this concentration we measured the volumes of the dilute phase ( $V'$ ), the concentrated phase ( $V''$ ), and the concentration of the dilute phase ( $c'$ ). The concentration  $c''$  is calculated from ( $c_t$  is the overall concentration)

$$c'' = V''^{-1} \{ c_t (V' + V'') - c' V' \}. \quad [1]$$

Due to experimental errors in the volumes  $V'$  and  $V''$  (especially when  $V''$  is small) and  $c'$  (when  $c_t$  and  $c'$  are nearly equal) the error in  $c''$  can be rather large. The volumes are calculated from the height of the phases and the diameter of the cuvettes. The height is measured with an accuracy of 0.5 mm using a sliding caliper.

### 3.6. Results

For the reasons outlined above, we cooled the samples twice and measured the volumes of both phases and the turbidity of the dilute

phase. The results for the systems studied (SE2 and SJ9 in toluene, SJ4 in benzene) are presented in Figs. 5, 6, and 7, where the concentration of the dilute and the concentrated phase is plotted on the horizontal axis and the temperature on the vertical axis. To obtain a clear picture we give the points for a few overall concentrations only. In Fig. 5 the experimental errors are shown as well (for one overall concentration). The experimental data (for SJ9) are represented in a different way in Fig. 8, where the concentration of the dilute phase is plotted as a function of overall concentration. In Fig. 9 the ratio of the volumes of the concentrated and the dilute phase of SJ9 is plotted as a function of overall concentration.

### 3.7. Fractionation

The silica particles are not completely monodisperse but are of various sizes (Table I). It is probable that the dispersability of the smaller particles within this distribution differs from that of the larger ones. Upon phase separation some fractionation by size may take place. This effect is investigated by measuring the (mean) radius of the particles taken from the dilute phase by TEM and comparing this radius with that of the original particles. This is done for three temperatures and three overall concentrations for the system SJ9 in toluene. The results are given in Table III.

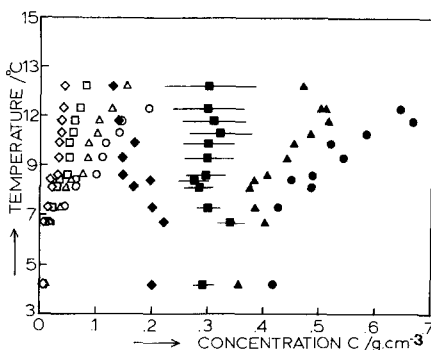


FIG. 5. Experimental phase diagram of SE2 in toluene. Some experimental errors are plotted.  $\diamond$ ,  $\blacklozenge$ ,  $c_t = 0.050$ ;  $\square$ ,  $\blacksquare$ ,  $c_t = 0.108$ ;  $\triangle$ ,  $\blacktriangle$ ,  $c_t = 0.208$ , and  $\circ$ ,  $\bullet$ ,  $c_t = 0.371$   $\text{g} \cdot \text{cm}^{-3}$ . Open symbols represent the dilute phase, filled symbols represent the concentrated phase.

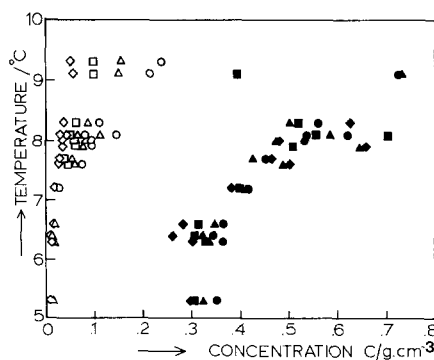


FIG. 6. Experimental phase diagram of SJ9 in toluene,  $\diamond$ ,  $\blacklozenge$ ,  $c_t = 0.057$ ;  $\square$ ,  $\blacksquare$ ,  $c_t = 0.106$ ;  $\triangle$ ,  $\blacktriangle$ ,  $c_t = 0.179$ , and  $\circ$ ,  $\bullet$ ,  $c_t = 0.273$   $\text{g} \cdot \text{cm}^{-3}$ . Open symbols represent the dilute phase, filled symbols represent the concentrated phase.

## 4. DISCUSSION

Attraction between particles in a solvent may be caused by the London-Van der Waals forces. These forces are determined to a great extent by the difference in the polarizability and thus in the refractive index of particles and solvent ( $n_{\text{particle}} \approx 1.43$ ). In Table I the cloud-point temperature is given along with the refractive index. It can be seen that there is no real correlation between the two; therefore it can be concluded that the instability does not originate solely in the London-Van der Waals forces. Calculation of these forces

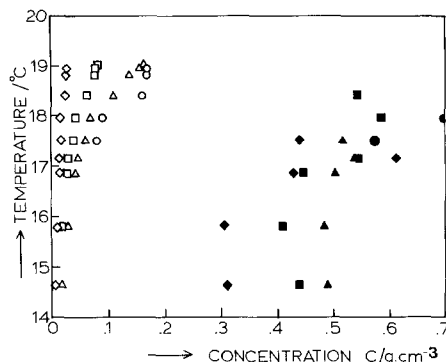


FIG. 7. Experimental phase diagram of SJ4 in benzene.  $\diamond$ ,  $\blacklozenge$ ,  $c_t = 0.030$ ;  $\square$ ,  $\blacksquare$ ,  $c_t = 0.103$ ;  $\triangle$ ,  $\blacktriangle$ ,  $c_t = 0.204$ , and  $\circ$ ,  $\bullet$ ,  $c_t = 0.399$   $\text{g} \cdot \text{cm}^{-3}$ . Open symbols represent the dilute phase, filled symbols represent the concentrated phase.

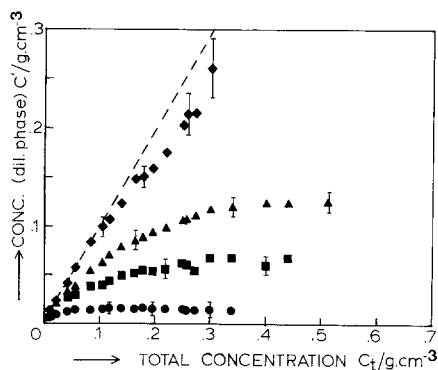


FIG. 8. Concentration of the dilute phase as a function of initial overall concentration for the system SJ9 in toluene. Data are shown for temperatures, ●, 6.3°C; ■, 7.7°C; ▲, 8.3°C; and ◆, 9.1°C. Some experimental errors are included.

between the particle cores (6) shows that they are indeed far too small to induce phase separation at ordinary temperatures. When the temperature approaches the critical temperature of the solvent the London–Van der Waals forces may become important, especially with large particles, as is concluded in Ref. (8).

In our case the origin of the instability is the bad quality of the solvent with regard to the stabilizing octadecyl chains. Therefore we compared the instability temperature with the Hildebrand solubility parameter of the solvent.

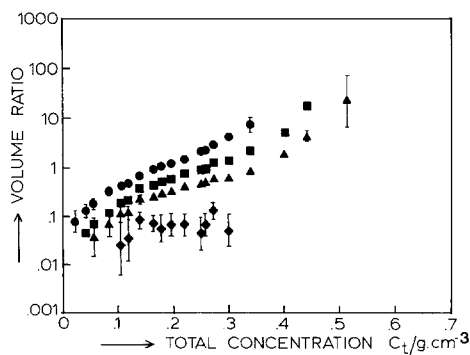


FIG. 9. The ratio of volumes of concentrated and dilute phase as a function of initial overall concentration for the system (SJ9) in toluene. Temperatures are the same as in Fig. 8.

TABLE III

Fractionation of Particles (SJ9) by Phase Separation

Temperature (°C)	$\alpha(t)$ ( $\text{g} \cdot \text{cm}^{-3}$ )		
	0.020	0.099	0.304
9.05	0.946	0.944	0.916
7.1	0.939	0.934	0.926
4.7	0.978	0.903	0.910

Note. The mean size of the particles in the dilute phase relative to the unfractionated mean size is given.

The solubility parameter of the chains on the particle is not known, but presumably does not differ much from that of octadecane ( $7.9$  ( $\text{cal}/\text{cm}^3$ )<sup>1/2</sup>). Solvents with about the same solvent parameter should be good solvents. When the difference increases the solvent quality deteriorates and instability occurs at a higher temperature. It can be seen however that the instability temperature does not depend in a straightforward way on the solubility parameter.

One can however notice certain subtrends, e.g., the solvent quality improves from benzene via toluene to xylene or ethyl benzene. Such a trend is seen with aliphatic polymers (e.g., PIB); also (12). In the series of the *n*-alkanes there is a clear dependence on chain length, the longer chains being poorer solvents than the shorter ones. A speculative explanation is that the instability is caused by an “induced freezing” of the solvent which can be deduced from the correlation between the freezing temperature of the solvent and the instability temperature. The solvent molecules are aligned by the densely packed octadecyl chains on the particle surface and therefore the structure of the solvent near the particle resembles a crystalline state of the solvent. The gel-like appearance may be due to the bridging of particles by solvent molecules absorbed in the layers of the particles. The fact that branched and cyclic alkanes show a lower transition temperature than linear alkanes supports the idea of bridging.

We observed that the concentrated phase decreased in volume when cooled slowly. A possible reason for this behavior is that the attractive forces between the particles increase strongly at decreasing temperatures. The particles then stick together in a loose gel-like network and the dispersion does not reach equilibrium. When the dispersion is cooled slowly it will probably be closer to equilibrium. However equilibrium is not reached completely, as can be concluded from the decrease in the volume of the concentrated phase when it is cooled for a second time. These effects are important when the temperature is well below the cloud-point temperature. It is therefore not certain whether equilibrium has been established at these low temperatures in the diagram.

When the phase diagrams of the different silica systems used are compared it becomes clear that the smaller particles are slightly more soluble than the large ones. The highest phase separation temperature observed for SJ9 is 9.3°C and for SE2 is 12.2°C. For SJ4 in toluene phase separation takes place at temperatures lower than -5°C. These observations are consistent with the idea that the smaller particles are less attractive because there are fewer chain contacts. The fractionation experiments (Table III) also show the better dispersibility of the smaller particles.

The phase diagrams show a clear dependence on overall concentration. This is thought to be an effect of polydispersity, as has been predicted by theoretical calculations (6). The dependence on overall concentration is found with polydisperse polymers (13) as well. The dilute phase behaves more or less as expected on the basis of theoretical calculations. The polydispersity required (in the calculations) to predict a dependence on overall concentration, as was observed in experiments, is greater than the actual spread in size. The polydispersity however is not in size only, but also in the attractive parameter. This parameter is proportional to the volume of interpenetration between two particle layers, which for two spheres with radius  $a$  and in-

terpenetration depth  $\Delta$  is about equal to  $(\pi/2)\Delta^2a$ . Because  $\Delta$  is small, a small (absolute) variation in  $\Delta$  leads to a large (relative) variation in the volume of overlap. Moreover since the particles are not perfect spheres this volume is sensitive to small irregularities on the particle surface.

Although the errors in the concentration of the concentrated phase are large, the experimental phase diagrams are rather dissimilar to the theoretical ones. First, at a fixed overall concentration, the concentration of the concentrated phase is lower at low temperatures than at high temperatures. The reverse is expected from theory. Second, at a fixed temperature, the order of the curves is reversed; i.e., the lower overall concentrations result in a lower concentration of the concentrated phase than do the higher concentrations.

A possible reason for the unexpected dependence of the concentrated phase may be that the concentrations in the dilute phase have not been determined correctly. As can be seen from the fractionation experiments the dilute phase is enriched with the smaller particles which causes a lower turbidity than one would expect if no fractionation had taken place. Therefore a lower concentration is found in the dilute phase and a higher concentration in the concentrated phase. Because fractionation depends on the overall concentration and on the temperature it is difficult to account for the effects of fractionation on the experimental phase diagram. In fact one should use a different calibration curve for each overall concentration and temperature, but this is not feasible. To estimate the effects of fractionation we did theoretical calculations on a bimodal system (6), which gave the volume fractions of both particles in dilute and concentrated phase. For the dilute phase the scattered intensity was calculated. With this intensity and a (calculated) calibration curve the volume fraction in the dilute phase was found (in the same manner as in experiments). Together with the volumes of both phases this volume fraction gives the volume fraction of the concentrated phase. A comparison of this

volume fraction with the one obtained directly from the computer calculations gives the effect of fractionation. It is found that the observed phase diagrams cannot be explained in terms of fractionation.

For some temperatures and initial overall concentrations we also measured the concentration in the dilute phase by drying a known volume and weighing the silica. This concentration was then compared with the one obtained via turbidity experiments and shown in Fig. 10. One notices that turbidity yields a lower concentration. The calculated (Eq. [1]) concentration of the concentrated phase is plotted in this figure as well. Now the concentration of the concentrated phase is not dependent on separation temperature and overall concentration (within experimental error, which is still rather large), so its behavior in Figs. 5, 6, and 7 is explained partly by the false estimate of the concentration on the basis of turbidity. However there is still a discrepancy between experiment and theoretical prediction.

Another reason for the unexpected behavior of the concentrated phase may be that this phase does not reach complete equilibrium. Especially at low temperatures the attractions between the particles are strong (larger than a few  $kT$ ). Therefore the particles cannot move freely. The dispersion resembles a glass, i.e.,

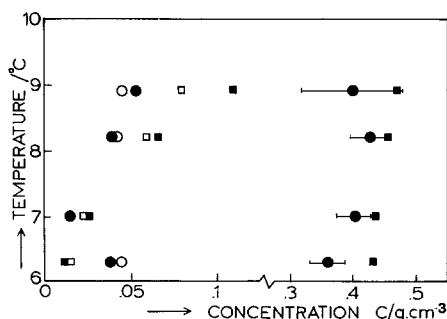


FIG. 10. Phase diagram of SJ9 in toluene obtained by measuring the concentration by weight for initial overall concentrations of (○, ●) 0.079 and (□, ■) 0.186  $\text{g} \cdot \text{cm}^{-3}$ . Concentration of the dilute phase as measured by means of turbidity is given by open symbols.

the structure is that of a liquid but the system hardly flows. In this structure solvent is trapped, which results in a larger volume and a low concentration.

We will now briefly compare our results with the ones of Edwards *et al.* (8). In the series of *n*-alkanes they found, on cooling the dispersions, the same trend in the instability temperature. They conclude, as we do, that the origin of the attraction upon cooling is not the London–Van der Waals forces between the particle cores, but is more an effect of the properties of the chains. The variation of the instability temperature as a function of particle size, the smaller particles being the most stable, is also found in Ref. (8). It is concluded in Ref. (8) that the separation is a spinodal decomposition, since the equilibrium concentrations and the (upper) flocculation do not coincide. We think that this discrepancy may be attributed to an effect of the polydispersity, such as depicted in Figs. 6–8. A spinodal decomposition is not likely, since the particles easily adhere to the walls of the container and thus form a kind of nucleus leading to binodal decomposition. The appearance of “embryo” clusters before actual phase separation occurs is, in our opinion, the onset of the attraction. This leads to thermodynamic (temporal) clusters and thus to an increase of turbidity. This effect is studied and described in more detail in Ref. (14).

## 5. CONCLUSION

From the results presented in this article it is clear that our silica particles do show a distinct and reversible phase separation when the dispersion is cooled. For these small particles coated with short chains the temperature range from stable to completely separated extends over 5–10 degrees, which is more than with large polymer coated particles (3, 5). However there is not a clear relation between the stability of the particles and the solubility parameter of the solvent. This relation is more evident with particles coated with polymer molecules like polyisobutene ( $M \approx 1500$ ), for

which results will be published. The cloud-point temperature also depends on concentration. This is because the loss in entropy for low concentrations is larger than for high concentrations and therefore a lower temperature is necessary to induce separation. The concentration of the phases depends on the initial concentration of the dispersion. This phenomenon can be explained in terms of polydispersity.

Further study is needed to investigate the concentration in the concentrated phase and with the probable nonequilibrium behavior at low temperatures. It is evident that attractions are present before separation occurs. Measurements of the attraction in the stable region will be reported in subsequent articles. Phase separation induced by temperature increase will be studied too.

#### ACKNOWLEDGMENTS

The authors thank Mr. E. Pelssers for preparing and characterizing one of the samples, Mr. P. Rouw for measuring the data of Fig. 10, and Mr. J. Pieters for taking the electron micrographs.

#### REFERENCES

1. van Helden, A. K., and Vrij, A., *J. Colloid Interface Sci.* **78**, 1618 (1981).
2. Kops-Werkhoven, M. M., and Fijnaut, H. M., *J. Chem. Phys.* **74**, 1618 (1981).
3. Napper, D. H., *J. Colloid Interface Sci.* **58**, 390 (1980).
4. Sato, T., and Ruch, R. (Eds.), "Stabilization of Colloid Dispersions by Polymer Adsorption," Surfactant Science Series, Vol. 9. Dekker, New York, 1980.
5. Cowell, C., Lin-In-On, R., and Vincent, B., *J. Chem. Soc. Faraday Trans. 1* **74**, 337 (1977).
6. Jansen, J. W., de Kruif, C. G., and Vrij, A., *J. Colloid Interface Sci.* **114**, 471 (1986).
7. Jansen, J. W., de Kruif, C. G., and Vrij, A., *Chem. Phys. Lett.* **107**, 450 (1984).
8. Edwards, J., Everett, D. H., O'Sullivan, T., Pangalou, I., and Vincent, B., *J. Chem. Soc. Faraday Trans. 1* **80**, 2599 (1984).
9. van Helden, A. K., Jansen, J. W., and Vrij, A., *J. Colloid Interface Sci.* **81**, 354 (1981).
10. Reynolds, W. W., "Physical Chemistry of Petroleum Solvents." Reinhold, New York, 1963.
11. Barton, A. F. M., *Chem. Rev.* **75**, 731 (1975).
12. Bandrup, J., and Immergut, E. H. (Eds.), "Polymer Handbook." Wiley, New York, 1977.
13. Koningsveld, R., and Staverman, A. J., *Kolloid Z. Z. Polym.* **218**, 194 (1967).
14. Jansen, J. W., de Kruif, C. G., and Vrij, A., *J. Colloid Interface Sci.* **114**, 492 (1986).